Electronic Supplementary Material (ESI) for Physical Chemistry Chemical Physics.

Probing the structural and electronic response of Magnus green salt compounds $[Pt(NH_2R)_4][PtCl_4]$ (R=H, CH_3) to pressure.

Jonathan G. Richardson,[a] Helen Benjamin,[a] Stephen A. Moggach,[b]* Lisette R. Warren,[a] Mark R. Warren,[c] David R. Allan,[c] Lucy Saunders,[c] Carole A. Morrison,[a]* and Neil Robertson[a]*

[a] *EaStCHEM School of Chemistry, University of Edinburgh, Edinburgh, UK*
[b] *Centre for Microscopy, Characterisation and Analysis, University of Western Australia, Australia*
[c] *Diamond Light Source, Diamond House, Harwell Science & Innovation Campus, Didcot, Oxfordshire, OX11 0DE, UK*

Contents **Page**

All crystallographic data have been deposited with the CCDC (CCDC 2009951-2009968) and can be obtained free of charge via https://www.ccdc.cam.ac.uk/structures/, or from the Cambridge Crystallographic Data Centre, 12 Union Road, Cambridge CB2 1EZ, UK (fax +441223336033; email deposit@ccdc.cam.ac.uk).

X-ray diffraction

Table S1: Crystallographic information for all the $MagNH_3$ structures in the pressure series.

	$MagNH_3$ at ambient conditions	**$MagNH_3$ at 0.37 GPa**	**$MagNH_3$ at 0.74 GPa**	**$MagNH_3$ at 1.06 GPa**	**$MagNH_3$ at 1.65 GPa**
Unit cell parameters	a = 8.97809(14) Å	a = 8.9435(5) Å	a = 8.8963(4) Å	a = 8.8591(6) Å	a = 8.7949(6) Å
	b = 8.97809(14) Å	b = 8.9435(5) Å	b = 8.8963(4) Å	b = 8.8591(6) Å	b = 8.7949(6) Å
	c = 6.4585(3) Å	c = 6.4253(7) Å	c = 6.3753(6) Å	c = 6.3339(8) Å	c = 6.2730(8) Å
	α = 90°	α = 90°	α = 90°	α = 90°	α = 90°
	β = 90°	β = 90°	β = 90°	β = 90°	β = 90°
	γ = 90°	γ = 90°	γ = 90°	γ = 90°	γ = 90°
	V = 520.59(3) Å^3	V = 513.93(6) Å^3	V = 504.57(4) Å^3	V = 497.11(6) Å^3	V = 485.22(6) Å^3
Space Group	*P4/mnc*	*P4/mnc*	*P4/mnc*	*P4/mnc*	*P4/mnc*
Wavelength [Å]	1.54178 (Cu Kα)	0.4859 (synchrotron)	0.4859 (synchrotron)	0.4859 (synchrotron)	0.4859 (synchrotron)
Completeness	99.7%	82.9%	75.4%	81.0%	82.6%
Resolution [Å]	0.84	0.85	0.85	0.85	0.85
R1	0.056	0.039	0.111	0.125	0.101

	$MagNH_3$ at 1.96 GPa	**$MagNH_3$ at 2.28 GPa**	**$MagNH_3$ at 2.71 GPa**	**$MagNH_3$ at 3.73 GPa**	**$MagNH_3$ at 4.62 GPa**
Unit cell parameters	a = 8.7712(8) Å	a = 8.7425(7) Å	a = 8.7220(11) Å	a = 8.6538(10) Å	a = 8.6076(14) Å
	b = 8.7712(8) Å	b = 8.7425(7) Å	b = 8.7720(11) Å	b = 8.6538(10) Å	b = 8.6076(14) Å
	c = 6.2436(9) A	c = 6.2161(8) Å	c = 6.1933(11) Å	c = 6.1220(12) Å	c = 6.0602(17) Å
	α = 90°	α = 90°	α = 90°	α = 90°	α = 90°
	β = 90°	β = 90°	β = 90°	β = 90°	β = 90°
	γ = 90°	γ = 90°	γ = 90°	γ = 90°	γ = 90°
	V = 480.35(7) Å^3	V = 475.10(6) Å^3	V = 471.14(8) Å^3	V = 458.47(9) Å^3	V = 449.01(12) Å^3
Space Group	*P4/mnc*	*P4/mnc*	*P4/mnc*	*P4/mnc*	*P4/mnc*
Wavelength [Å]	0.4859 (synchrotron)	0.4859 (synchrotron)	0.4859 (synchrotron)	0.4859 (synchrotron)	0.4859 (synchrotron)
Completeness	83.2%	82.9%	82.8%	82.4%	83.1%
Resolution [Å]	0.85	0.85	0.85	0.85	0.85
R1	0.089	0.095	0.087	0.110	0.086

Table S2: Crystallographic information for all the $MagNH_2Me$ structures in the pressure series.

	$MagNH_2Me$ at ambient	**$MagNH_2Me$ at 0.16 GPa**	**$MagNH_2Me$ at 0.25 GPa**	**$MagNH_2Me$ at 0.58 GPa**	**$MagNH_2Me$ at 0.90 GPa**

	conditions				
Unit cell parameters	a = 10.35151(12) Å	a = 10.3266(8) Å	a = 10.3078(8) Å	a = 10.2482(7) Å	a = 10.1964(7) Å
	b = 10.35151(12) Å	b = 10.3266(8) Å	b = 10.3078(8) Å	b = 10.2482(7) Å	b = 10.1964(7) Å
	c = 6.4977(2) Å	c = 6.4805(10) Å	c = 6.4712(10) Å	c = 6.4309(9) Å	c = 6.3876(9) Å
	α = 90°	α = 90°	α = 90°	α = 90°	α = 90°
	β = 90°	β = 90°	β = 90°	β = 90°	β = 90°
	γ = 90°	γ = 90°	γ = 90°	γ = 90°	γ = 90°
	V = 1281.43(7) Å^3	V = 691.06(10) Å^3	V = 687.57(11) Å^3	V = 675.41(10) Å^3	V = 664.10(9) Å^3
Space Group	*P4/mnc*	*P4/mnc*	*P4/mnc*	*P4/mnc*	*P4/mnc*
Wavelength [Å]	1.54178 (Cu Kα)	0.4859 (synchrotron)	0.4859 (synchrotron)	0.4859 (synchrotron)	0.4859 (synchrotron)
Completeness	96.7%	89.5%	93.1%	92.0%	97.2%
Resolution [Å]	0.80	0.84	0.84	0.84	0.84
R1	0.050	0.056	0.050	0.057	0.029

	$MagNH_2Me$ at 1.23 GPa	**$MagNH_2Me$ at 1.61 GPa**	**$MagNH_2Me$ at 1.92 GPa**	**$MagNH_2Me$ at 2.33 GPa**
Unit cell parameters	a = 10.1452(13) Å	a = 10.0908(14) Å	a = 10.056(2) Å	a = 14.160(9) Å
	b = 10.1452(13) Å	b = 10.0908(14) Å	b = 10.056(2) Å	b =14.179(3) Å
	c = 6.3581(11) Å	c = 6.3306(17) Å	c = 6.320(3) Å	c =6.274(1) Å
	α = 90°	α = 90°	α = 90°	α = 90°
	β = 90°	β = 90°	β = 90°	β = 92.13(3)°
	γ = 90°	γ = 90°	γ = 90°	γ = 90°
	V = 654.41(11) Å^3	V = 644.60(18) Å^3	V = 639.1(3) Å^3	V = 1258.79 Å^3
Space Group	*P4/mnc*	*P4/mnc*	*P4/mnc*	*C2/c*
Wavelength [Å]	0.4859 (synchrotron)	0.4859 (synchrotron)	0.4859 (synchrotron)	0.4859 (synchrotron)
Completeness	96.6%	98.4%	82.8%	58.0 %
Resolution [Å]	0.84	0.84	0.84	0.80
R1	0.043	0.050	0.041	Structure Unsolved

Table S3: Selected bond length and torsion angles in $MagNH_3$ throughout the pressure series.

Pressure (GPa)	Pt–N bond length (Å)	Pt–Cl bond length (Å)	Cl–Pt···Pt–N torsion angle (°)
Ambient	2.068(10)	2.330(4)	-29.1(2)
0.37	2.058(8)	2.332(3)	-28.4(2)
0.74	2.064(12)	2.324(4)	-28.1(3)
1.06	2.069(13)	2.329(4)	-28.9(3)
1.65	2.061(14)	2.320(4)	-28.5(4)
1.96	2.079(18)	2.321(6)	-28.6(4)
2.28	2.066(18)	2.315(5)	-28.9(5)
2.71	2.069(17)	2.323(5)	-29.0(4)
3.73	2.074(18)	2.318(6)	-30.1(5)
4.62	2.050(30)	2.321(9)	-29.3(7)

Table S4: Selected bond lengths, bond angles, and torsion angles in $MagNH_2Me$ throughout the pressure series.

Pressure (GPa)	Pt–N bond length (Å)	Pt–Cl bond length (Å)	∠Pt–N–C angle (°)	Cl–Pt···Pt–N torsion angle (°)
Ambient	2.059(10)	2.320(3)	124.0(8)	31.3(2)
0.16	2.089(11)	2.329(3)	124.2(8)	32.5(3)
0.25	2.087(9)	2.325(3)	123.2(7)	32.3(2)
0.58	2.079(12)	2.326(4)	124.5(9)	33.5(3)
0.90	2.095(14)	2.321(4)	122.7(12)	32.6(3)
1.23	2.066(13)	2.309(5)	124.0(11)	33.4(3)
1.61	2.059(11)	2.303(5)	125.6(10)	33.8(3)
1.92	2.109(19)	2.316(6)	124.2(14)	33.4(4)

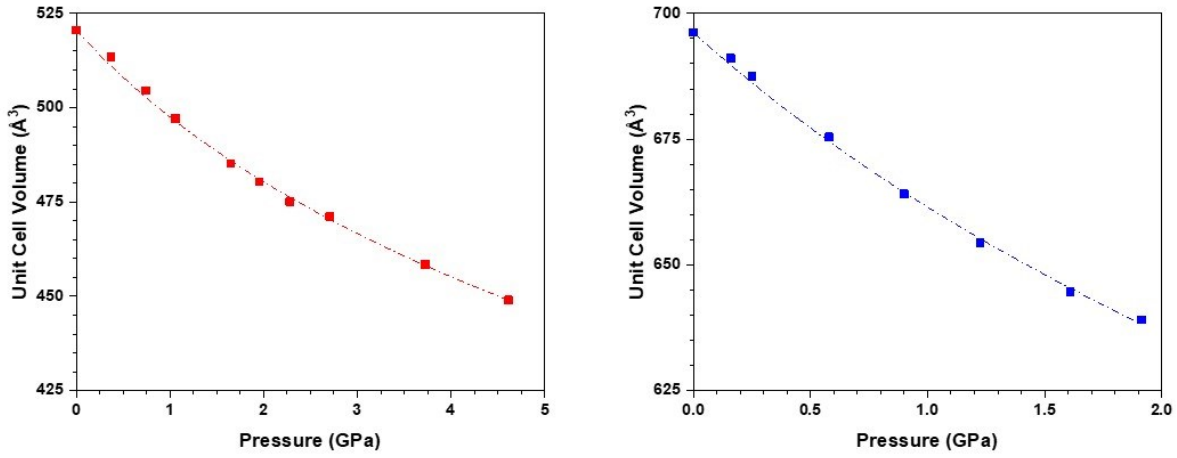

Figure S1: Graph of unit cell volume compression of $MagNH_3$ (left) and $MagNH_2Me$ (right) (prior to the phase transition), with their respective 3rd order Birch-Murnaghan equation of state plots.[1]

Solid state calculations

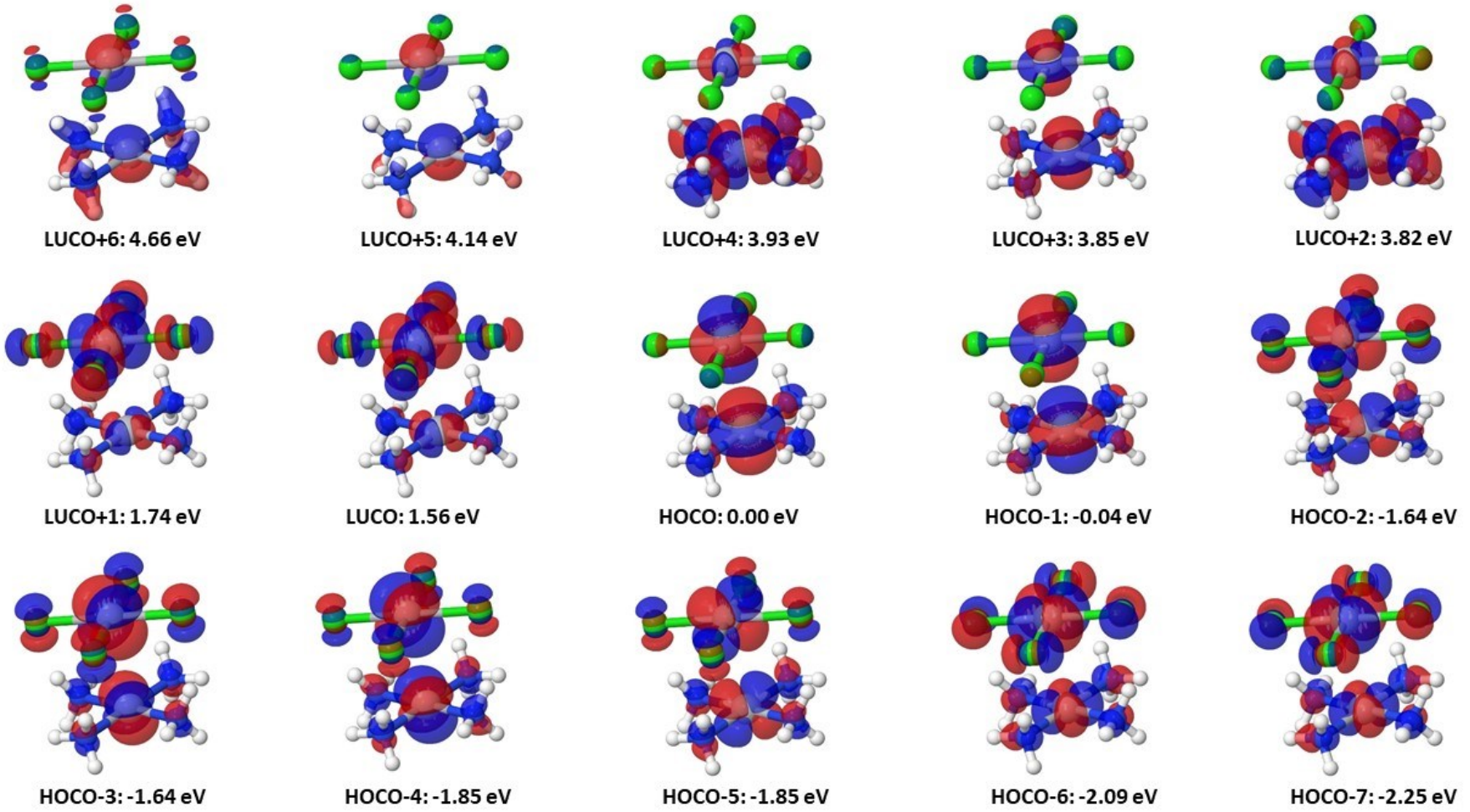

Figure S2: Crystalline orbitals of bands either side of the band gap for $MagNH_3$, obtained at the Γ k-point. Atoms are coloured: Cl, green; Pt, grey; N, blue; H, white.

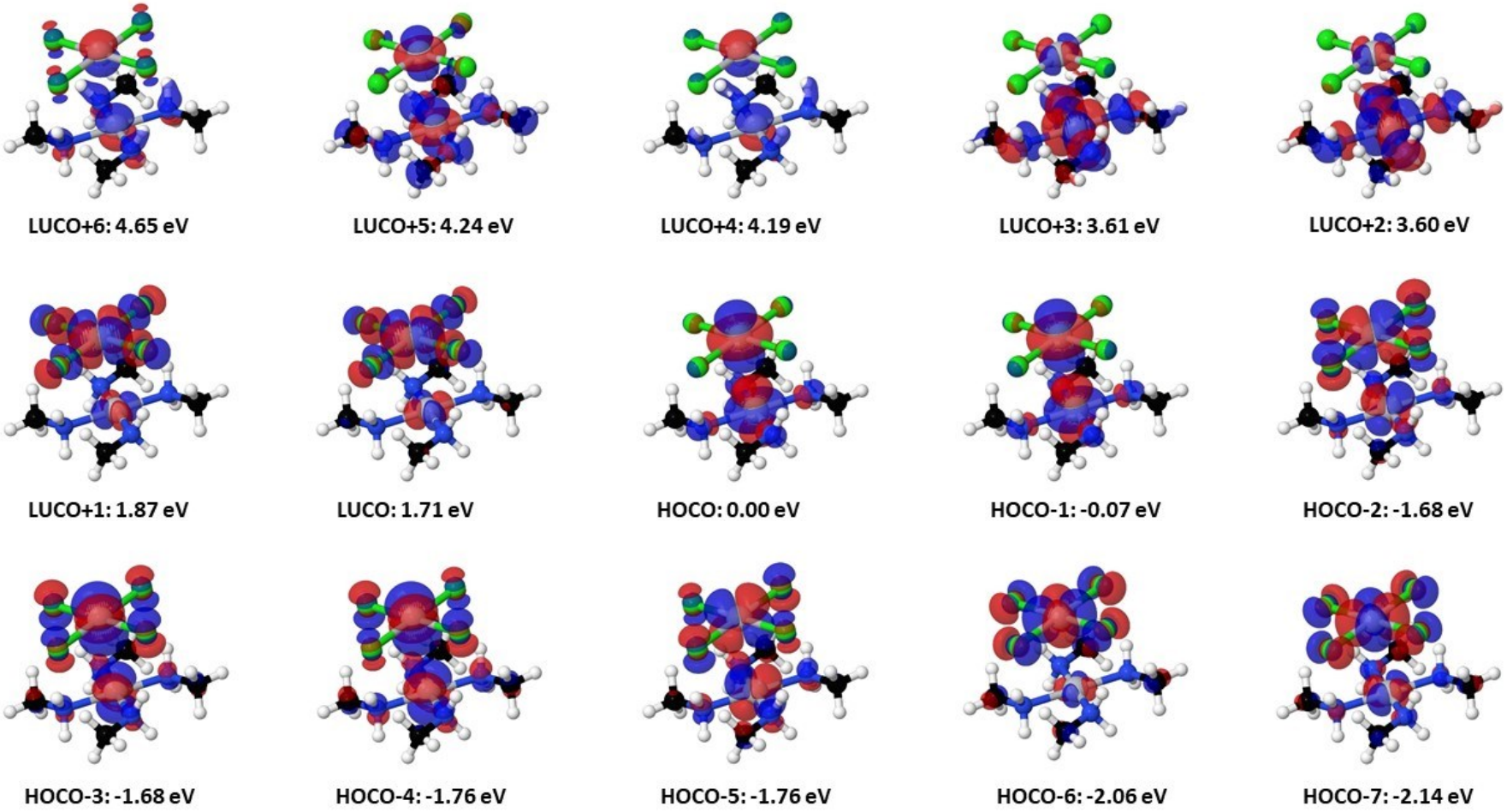

Figure S3: Crystalline orbitals representing band either side of the band gap for $MagNH_2Me$, obtained at the Γ k-point. Atoms are coloured: Cl, green; Pt, grey, N; blue, C, dark grey; H, white.

While, as illustrated in the main text (Figures 3 and 5), the majority of the LUCO band for both $MagNH_3$ and $MagNH_2Me$ consists of contributions from anti-bonding Pt···Cl and, to a much lesser extent, Pt···N interactions, weak Pt···Pt interactions were also observed. Figures S4 and S5 show the COHP plot of only the Pt···Pt interaction contribution to the LUCO band for $MagNH_3$ and $MagNH_2Me$ respectively throughout their respective pressure series; the ambient position of the LUCO and LUCO+1 bands are provided alongside the related electronic band structure to act as a reference point. The Pt···Pt interaction in $MagNH_3$ LUCO is weakly bonding whilst the interaction in the LUCO band of $MagNH_2Me$ is weakly anti-bonding. The difference in nature of this interaction stems from the subtle difference in the Pt orbital overlap caused by the different intra-chain Cl-Pt···Pt-N dihedral angles in the two compounds, and thus is attributed as a cause for the slightly larger band gap at ambient conditions for $MagNH_2Me$, decreasing or increasing the LUCO energy for $MagNH_3$ and $MagNH_2Me$ respectively from its average position if there was no Pt···Pt interaction.

The magnitude of this interaction gets stronger throughout the pressure series for both compounds. Therefore, for $MagNH_3$, the result of the strengthening this Pt···Pt interaction results in a slight stabilisation of the LUCO, whereas it causes a slight destabilisation of the LUCO of $MagNH_2Me$; these can be seen in Figures S4, S5 and S8.

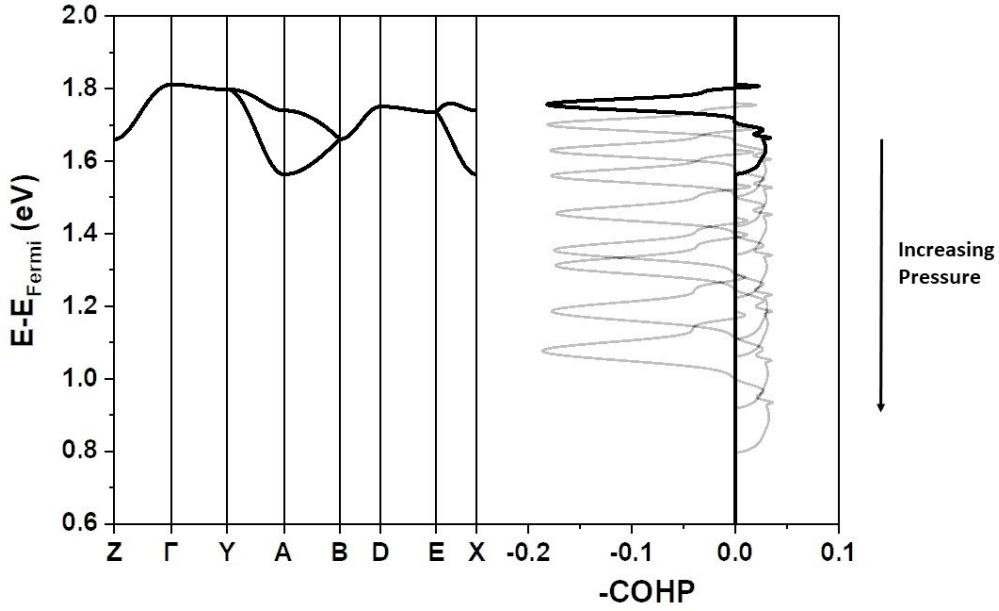

Figure S4: -COHP plot of Pt…Pt interaction in $MagNH_2Me$, ranging from low to high pressure (signified by the increasing transparency of the line plots) structures throughout the pressure series, in the energy range associated with the LUCO and LUCO+1 bands.

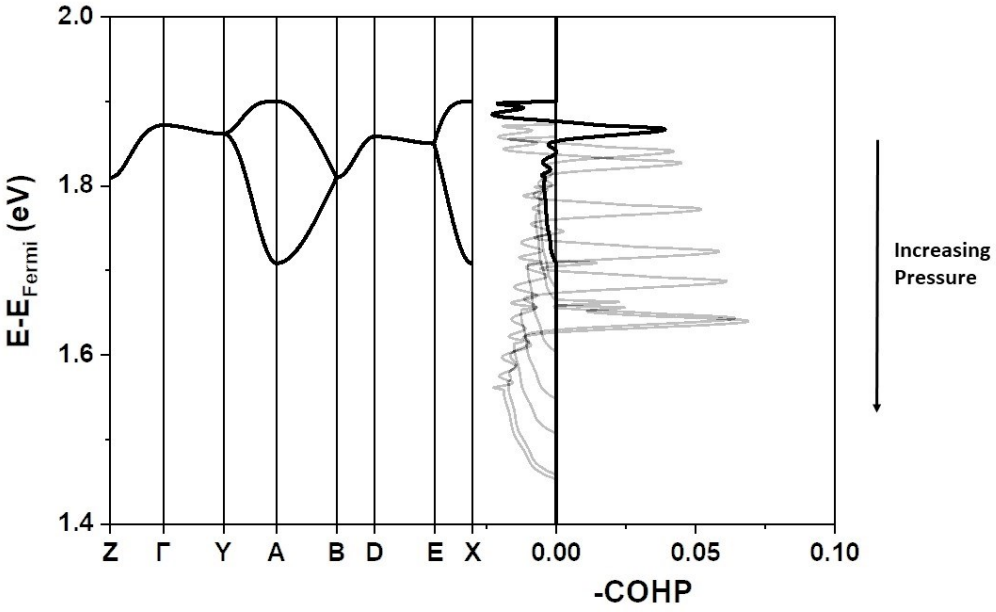

Figure S5: -COHP plot of Pt···Pt interaction in $MagNH_3$, ranging from low to high pressure (signified by the increasing transparency of the line plots) structures throughout the pressure series, in the energy range associated with the LUCO and LUCO+1 bands.

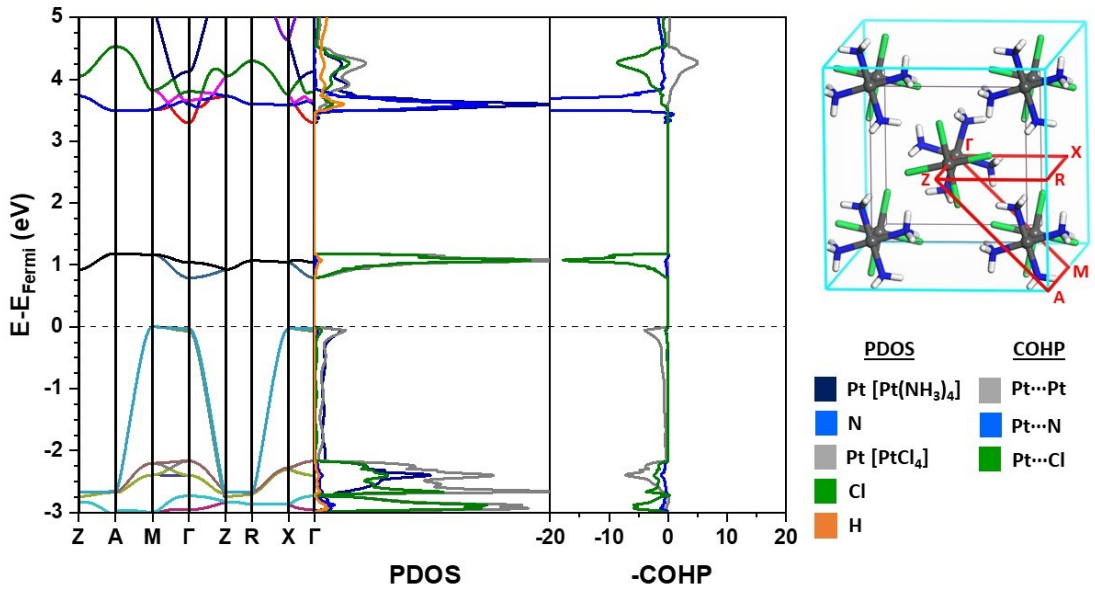

Figure S6: LEFT: Electronic band structure, projected density of states (PDOS) and COOP plot of the structure of $MagNH_3$ obtained experimentally at 4.62 GPa. RIGHT: Real space (grey) and reciprocal (light blue) lattices of $MagNH_2Me$, with the Brillouin zone path used in the electronic band structure coloured in red. E_{Fermi} = -4.141 eV.

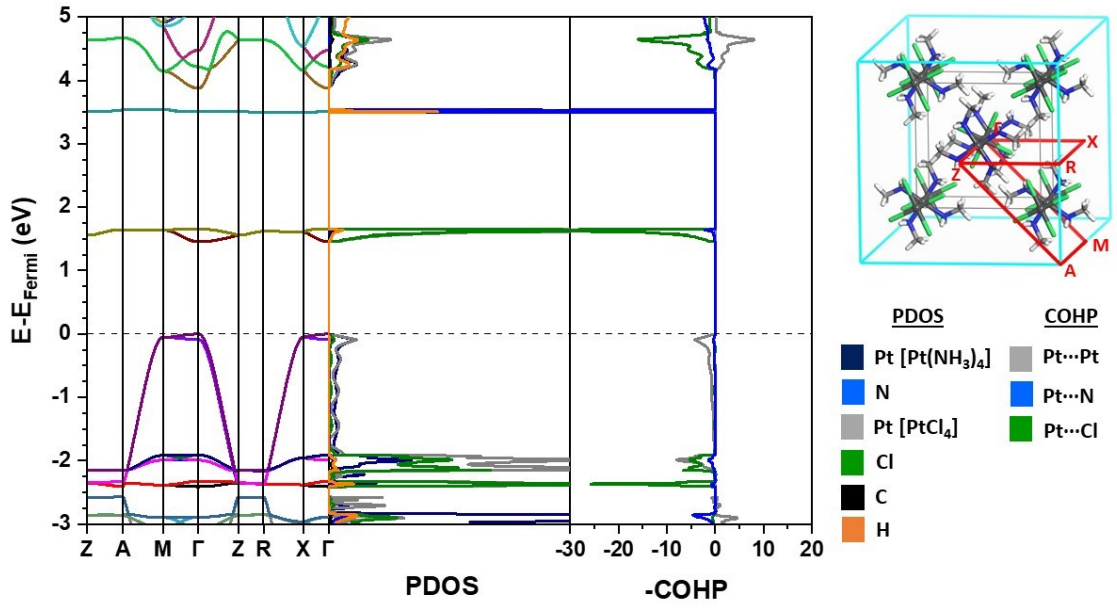

Figure S7: LEFT: Electronic band structure, projected density of states and -COHP plot (left) of the 1.61 GPa structure of $MagNH_2Me$. RIGHT: Real space (grey) and reciprocal (light blue) lattices of $MagNH_2Me$, with the Brillouin zone path used in the electronic band structure coloured in red. E_{Fermi} = -4.348 eV.

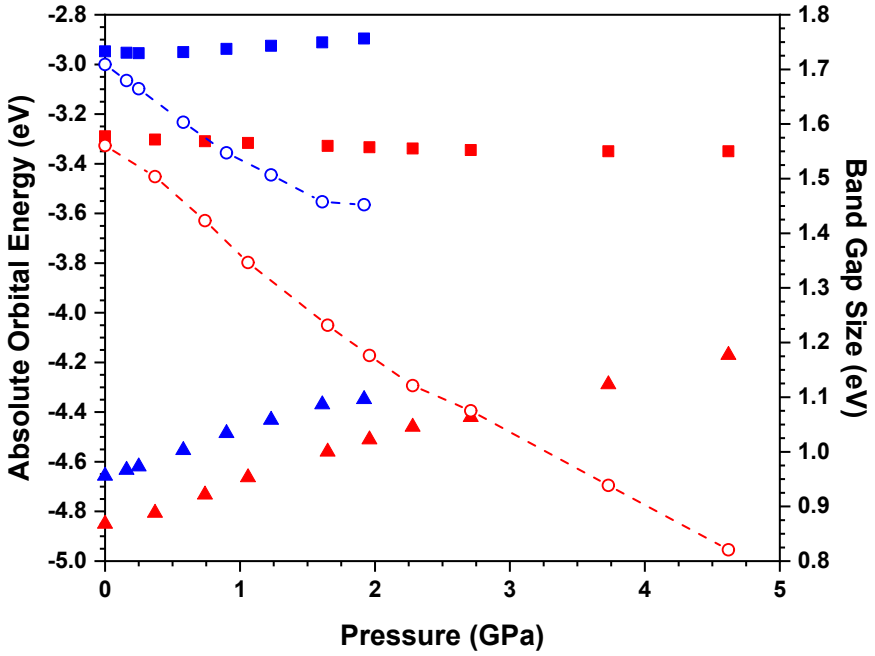

Figure S8: Absolute energies of the HOCO (triangle) and LUCO (square) across the entire pressure series for both $MagNH_3$ (red) and $MagNH_2Me$ (blue). The open circles indicate the band gap size for the two compounds, which is obtained by a subtraction of the HOCO and LUCO energy values.

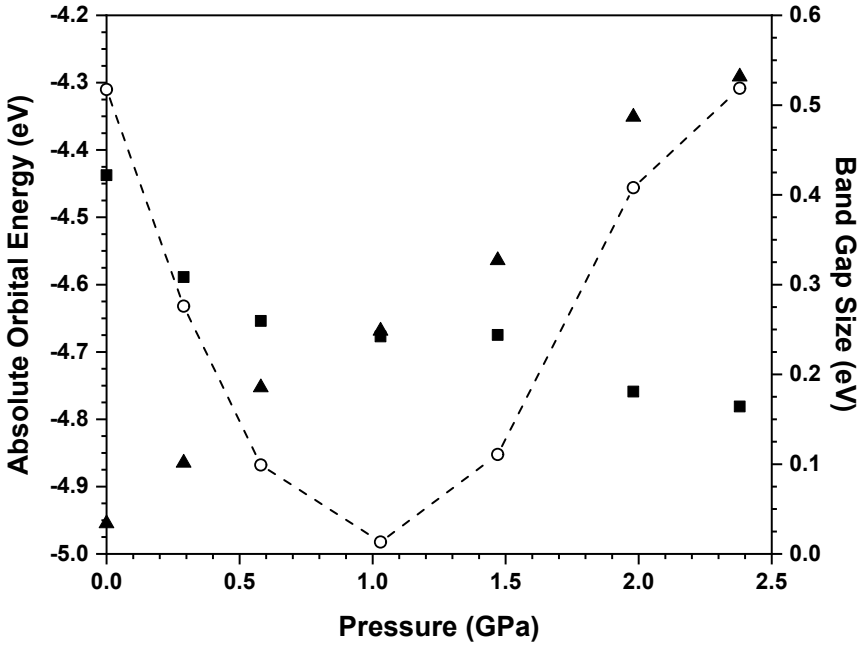

Figure S9: Absolute energies of the ambient pressure described HOCO (triangle) and LUCO (square) across the entire pressure series for $Pt(bqd)_2$.[2] The open circles indicate the band gap size for the two compounds, which is obtained by a subtraction of the HOCO and LUCO energy values.

Table S5: Calculated Pt-N and Pt-Cl bond lengths, with comparison to experimental values obtained in ambient pressure structure of $MagNH_3$ for range of functionals tested using atom only and full (atom and unit cell) optimisation methods.

Functional	Optimisation Method	Pt–N distance (Å)	% difference vs experimental	Pt–Cl distance (Å)	% difference vs experimental
PBE	Atom only	2.079	+4.4 %	2.417	+3.8 %
	Full	2.075	+4.2 %	2.464	+5.9 %
BLYP	Atom only	2.101	+5.5 %	2.455	+5.5 %
	Full	2.094	+5.1 %	2.498	+7.3 %
PBE0	Atom only	2.064	+3.6 %	2.394	+2.9 %
	Full	2.058	+3.3 %	2.390	+2.7 %
B3LYP	Atom only	2.084	+4.6 %	2.424	+4.2 %
	Full	2.078	+4.3 %	2.420	+4.0 %
HSE06	Atom only	2.067	+3.7 %	2.396	+3.0 %
	Full	2.060	+3.4 %	2.391	+2.8 %

Table S6: Calculated unit cell parameters from full (atom and until cell) geometry optimisations of the ambient structure of $MagNH_3$ for a range of functionals, compared to the experimental unit cell parameters.

Functional	*a* (Å)	% diff vs experimental	*c* (Å)	% diff vs experimental	Volume	% diff vs experimental
PBE	8.939128	-0.4 %	5.974672	-7.5 %	477.4241	-8.3 %
BLYP	8.919282	-0.7 %	5.994223	-7.2 %	476.862	-8.4 %
PBE0	8.839227	-1.6 %	6.201572	-4.0 %	484.5408	-6.9 %
B3LYP	8.851605	-1.4 %	6.232133	-3.5 %	488.2933	-6.2 %
HSE06	8.842312	-1.5 %	6.208547	-3.9 %	485.4244	-6.8 %

Table S7 Calculated electronic band gaps calculated for the structures of $MagNH_3$ (obtained at ambient conditions and 4.62 GPa) and $MagNH_2Me$ (obtained at ambient conditions and 1.61 GPa)

Structure	Functional	Optimisation	Ambient Pressure	Calculated	Average of	Predicted

		Method	Calculated Band Gap (eV)	High Pressure Band Gap (eV)	Rate of Band Gap Compression (eV GPa^{-1})	Pressure of Metallic State Formation (GPa)
$MagNH_3$	PBE	Atom-Only	0.029	0.000	-	-
		Full	0.000	-	-	-
	PBE0	Atom-Only	2.296	1.485	-0.18	13.08
		Full	1.805	-	-	-
	BLYP	Atom-Only	0.000	0.000	-	-
		Full	0.000	-	-	-
	B3LYP	Atom-Only	1.715	0.972	-0.16	10.66
		Full	1.315	-	-	-
	HSE06	Atom-Only	1.560	0.821	-0.16	9.75
		Full	1.116	-	-	-
$MagNH_2Me$	PBE	Atom-Only	0.153	0.000	-	-
	PBE0	Atom-Only	2.441	2.169	-0.17	-
	B3LYP	Atom-Only	1.851	1.646	-0.13	-
	HSE06	Atom-Only	1.709	1.458	-0.16	-

References

1. F. Birch, *Phys. Rev.*, 1947, **71**, 809-824.
2. H. Benjamin, J. G. Richardson, S. A. Moggach, S. Afanasjevs, L. Warren, M. R. Warren, D. R. Allan, C. A. Morrison, K. V. Kamenev and N. Robertson, *Phys. Chem. Chem. Phys.*, 2020, **22**, 6677-6689.